Characterizing two new *Henneguya* species in the respiratory organs of African Sharptooth Catfish

Walaa F. A. Emeish[1], Marwa M. Fawaz[2], Nermean M. Hussein[3], Zeinab Al-Amgad[4], Hanan H. Abd-ElHafeez*[5], Catrin Sian Rutland[6], and Karima A. Bakry[1]

[1]Fish Diseases and Management, Department of Fish Diseases, Faculty of Veterinary Medicine, South Valley University, Qena 83523, Egypt. ewalaa@vet.svu.edu.eg ; karima-alaa@vet.svu.edu.eg

[2]Department of Parasitology, Faculty of Veterinary Medicine, South Valley University, Qena, Egypt. m_abdallah@vet.svu.edu.eg

[3]Department of Zoology, Faculty of Science, South Valley University, Qena, Egypt. nermeanmohu@yahoo.com

[4]General Authority for Veterinary Services, Qena Veterinary Directorate, Qena, Egypt. zizi_1283@yahoo.com

[5]Department of Cell and Tissues, Faculty of Veterinary Medicine, Assiut University, Assiut, 71526, Egypt. hhnnzz91@aun.edu.eg

[6]School of Veterinary Medicine and Science, University of Nottingham, Nottingham, UK. Catrin.rutland@nottingham.ac.uk

* Correspondence author: Hanan H. Abd-ElHafeez. Department of Cell and Tissues, Faculty of Veterinary Medicine, Assiut University, Assiut, 71526, Egypt. hhnnzz91@aun.edu.eg

Abstract:

Henneguya species are myxozoans, a suborder of Cnidaria, which can affect the gills and extrarespiratory organs of the African sharptooth catfish, *Clarias gariepinus*. This research describes natural infection-induced histological alterations caused by the *Henneguya* species present. The *Henneguya* species were also identified molecularly using DNA sequenced from infected tissue cysts, and phylogenetically analyzed. Clinical investigations revealed cyst-like nodules on the fish gill filaments and extra respiratory organs. Within a milky fluid inside the cysts were several *Henneguya*-like spores. *Henneguya* sp. infested 27.5% of the fish, with the highest prevalence in the gills compared to the extra respiratory organs. The *Henneguya* species parasitized the gill, and the dendritic tissues, resulting in histopathological characteristics. The plasmodia's developmental stages resulted in destructive damage which manifested as marked necrosis, which was replaced by a focal aggregation of inflammatory cells. Amplification of the 18S ribosomal DNA from the fish parasites was followed by sequencing, which confirmed their identities as new species *Henneguya qenabranchiae* n. sp. and *Henneguya qenasuprabranchiae* n. sp. with 99.53 % and 99.64% identity, respectively, to *Henneguya* sp. 1 HS-2015. The two *C. gariepinus* myxozoans, shared some characteristics based on morphologic and phylogenetic analysis as previously published, where it was previously proposed that they were a sister lineage to *Henneguya* species in Egypt, it is now proposed that they are new species.

Keywords: *Clarias gariepinus*; Myxozoan; *Henneguya*; phylogenetic analysis

1. Introduction

Myxozoans are obligate parasites, and include a group of more than 2400 species from the Cnidaria phylum that have been described from fish studies (Eszterbauer et al., 2020). They are morphologically, and functionally, simplified organisms that share two-host life cycles, and most commonly utilize fish as intermediate hosts and oligochaete worms as definitive hosts (Stilwell et al., 2019). They are commonly parasitic in fish all over the world (Lom & Dyková, 1992), infecting nearly all classes of fish in all aquatic environments with remarkably variable tissue tropism. While most infections are harmless, some are dangerous and cause significant economic losses in freshwater, marine-cultured, and wild fish (Stilwell et al., 2019). However, due to convergence in myxospore morphologies, knowledge relating to host preference, tissue specificity, developmental features, and progressively molecular sequence data are needed for appropriate identification (Okamura et al., 2015). New species of myxosporeans are continually being identified and described and have been found to parasitize a wide variety of fish tissues.

The different *Henneguya* spp. infect a variety of tissues, including the gills and extra respiratory organs, but their initial descriptions were based on myxospore morphology. Most documented cases of *Henneguya* species affecting African sharptooth catfish in Egypt therefore have scarce data relating to the 18S small subunit rDNA gene sequence. Up until now, some work has identified *Henneguya* spp. infecting gills and extra respiratory organs using molecular methods and reported a phylogenetic clade for the *Henneguya* spp (Abdel-Ghaffar et al., 2015; Saleh, 2015). However, in situ studies linking sequence data from myxospores to specific tissue sites have not been well documented and remain a matter of speculation.

The present study describes the occurrence and identification of the respiratory form of henneguyosis in African sharptooth catfish, *C. gariepinus,* collected from the Nile River Branch in Qena Province. Our goals focused on: 1) identifying the morphological features and providing descriptions of histopathological changes induced by the myxozoan *Henneguya* spp. in both the gills and extra respiratory organs, and 2) confirming the presence of the parasite within lesions using myxozoan-specific PCR and sequencing, and supplementing these results with detailed phylogenetic analysis.

2. Materials and Methods

2.1 Sample collection

Wild African sharptooth catfish, *C. gariepinus* (n =120) were collected randomly from the Nile River at Qena Province (coordinates: 26° 10′ 12″ N 32° 43′ 38″ E), Egypt, by fishermen. Fish with an average weight of 250–700 g were transported immediately alive in fiberglass tanks to the Aquatic Diagnostic Laboratory, Faculty of Veterinary Medicine, South Valley University, Qena , and euthanized using clove oil (40 mg/l) prior to tissue sampling (Griffiths, 2000). The present study follows the ethical guidelines for animal experimentation and research at the South Valley University (RCOE-SVU-SSouth Valley University) and was approved by the Ethical Research Committee of the Faculty of Veterinary Medicine, South Valley University, Egypt, approval number (No.77/04.10.2022).

Clinical and parasitological examinations were performed on each fish. The gills and the extra respiratory organs were exposed and removed for additional examination in order to detect and identify the henneguyosis infestation, following the methods previously published (Noga, 2010). Fifteen samples were additionally taken from each gill and extra respiratory organ presenting with gross lesions, suggestive of *Henneguya* infection. The operculum was removed using scissors to expose the gills and extra respiratory organs. The tissue was then washed in saline solution and fixed in either 10% neutral buffered formalin for histopathological examination or 70% ethanol for molecular studies. Some of the fluid was extracted from each cyst, put on glass slides, and observed using light and scanning electron microscopes (SEM).

2.2 Parasitological, light, and SEM analysis

Fresh myxospores (n = 25), were measured (in μm) in accordance with a previously published method (Lom & Arthur, 1989) and the images of the detected fresh myxospores were photographed using a digital microscope (Leica Microsystems, CH-9435 Heebrugg, Ec3, Singapore). Thin films were formed from squashed preparations and the homogenized material was air-dried, fixed using absolute methyl alcohol.

These were dried then stained with Giemsa (pH 7.2) for 20 minutes, then left to dry at room temperature. The films were examined under an oil immersion lens.

The slides containing parasite spores from the gills and extra respiratory organs were fixed in 3.5% glutaraldehyde in phosphate buffer, pH 7.4, for 3-4 hours, then post-fixed in 1% osmium tetraoxide for 2 hours, washed with sodium-phosphate buffer (pH 7.4), dried, mounted on copper studs, and gold-coated (Emeish et al., 2022). The smears were examined using a JEOL JSM-5400LV SEM operating at 15 kV in the electron microscopy unit, South Valley University.

2.3 Histopathological analysis

Following the necropsies of both the parasitized and non-infected fish, fresh biopsies were immediately taken from the gills and extra respiratory organs and fixed in 10% neutral buffered formalin. Then, formalin-fixed samples were processed using traditional paraffin embedding techniques (Soliman et al., 2022a; Soliman et al., 2022b). Using methods reported by Bancroft & Gamble (2008), 5 µm paraffin sections were prepared and stained with hematoxylin and eosin (H&E), in preparation for observation using light microscopy and histopathological examination.

2.4 DNA extraction and amplification

Individual cysts were excised from the ethanol-fixed tissues and washed with sterile distilled water to remove any ethanol remnants. DNA was extracted from the cyst contents using a Qiagen QIAamp DNA Mini kit (Qiagen, Hilden, Germany) according to the manufacturer's protocols. A nested PCR reaction (nPCR) using previously published primers, targeting the universal eukaryotic primers (ERIB1 and ERIB10) (Barta et al., 1997) and a myxosporean specific 18S rDNA (MyxospecF and MyxospecR) (Fiala, 2006), was performed with some modifications to confirm the presence of *Henneguya* spp. in the fish. Briefly, 2 µl from the initial PCR products, generated using ERIB1 and ERIB10 primers, was added to 23 µl of master mix that included 12.5 µl 2× Reddy Mix PCR Master mix (Thermo Scientific, Hamburg, Germany), containing 75 mM Tris-HCl (pH 8.8), 20 mM $(NH_4)_2$ SO_4, 1.5 mM $MgCl_2$, 0.01% Tween-20, 0.2 mM of each nucleotide triphosphate, 1.25 U thermoprime plus DNA polymerase, and red dye for electrophoresis, and then 10 pmol each of forward and reverse primer (**Table 1**). The mixture was filled to a 25 µl end volume using nuclease-free water. The reaction was subjected to 35 amplification cycles of 95°C for 1 min, 52°C for 1 min, and 72°C for 2 min. These amplification cycles were preceded by an initial denaturation step at 95°C for 3 min and ended with a final extension step at 72°C for 10 min.

Table 1. Primers used for PCR amplification and sequencing of the small subunit rDNA gene from the myxospores.

Name	Sequences (5`-3`)	Amplicon size	References
MyxospecF	TTC TGC CCT ATC AAC TWG TTG	~ 850	**(Fiala, 2006)**
MyxospecR	GGT TTC NCD GRG GGM CCA AC		
ERIB1	ACC TGG TTG ATC CTG CCA G	1734-2142	
ERIB10	CTT CCG CAG GTT CAC CTA CGG		**(Barta et al., 1997)**

2.5. DNA sequencing and phylogenetic analysis

The PCR products were purified using a MinElute gel extraction kit (QIAGEN, Hilden, Germany), oligonucleotide synthesis and DNA nucleotide sequencing were performed by Macrogen *Humanizing Genomics* biotechnology company, Seoul, South Korea. The nucleotide sequences obtained were analysed using Basic Local Alignment Search Tool (BLASTn; http://www.ncbi.nlm.nih.gov/BLAST/) to establish sequence similarities (Altschul et al., 1997). Sequences with higher identities (>90% identity, and query cover >71%) were downloaded from the GenBank for phylogenetic analysis of the *Henneguya* sp. isolated from the

gills (**Table 2**). Likewise, sequences with high identities (>88% identity, and query cover >94%) were also downloaded from the GenBank for the phylogenetic analysis of *Henneguya* sp. isolated from the extra respiratory organs (**Table 3**). *Sphaerospora renicola* (GenBank accession number, JF758875) was used as an out-group species. Alignment using the Muscle tool and evolutionary analyses were done in Molecular Evolutionary Genetics Analysis, MEGA X software (https://www.megasoftware.net/) according to Kumar et al. (2018) and a phylogenetic tree using the Maximum Likelihood method was performed according to Tamura & Nei (1993). Bootstrap confidence values were calculated with 1000 repetitions. The analysis involved 15 (**Table 2**) and 14 (**Table 3**) nucleotide sequences for the phylogenetic tree of *Henneguya* spp. isolated from the gills and extra respiratory organs, respectively.

Table 2. *Myxospores* species > 90% identity, and query cover > 71% obtained from the GenBank and used for phylogenetic analysis of *H. qenabranchiae* n. sp. described in the present study.

Accession No.	Organism	Host origin	Infected organ	Locality
MT231728	*H. qenabranchiae* n. sp.	*C. gariepinus*	Gills	Egypt
KP990669	*Henneguya* sp. 1 HS 2015	*C. gariepinus*	Extra respiratory organs	Egypt
MT231731	*H. qenasuprabranchiae* n. sp	*C. gariepinus*	Extra respiratory organs	Egypt
KM000055	*Henneguya bulbosus*	*Ictalurus punctatus*	Intralamellar gill pseudocyst	USA
FJ468488	*Henneguya pellis*	*Ictalurus furcatus*	External/internal pseudocyst	USA
AF021881	*Henneguya exilis*	*Ictalurus punctatus*	Gills	USA
MT437047	*Henneguya* sp. k AC-2020	*Lates calcarifer*	Gills	India
MZ905346	*Henneguya sutherlandi*	*Ictalurus punctatus*	Gills	USA
EF191200	*Henneguya sutherlandi*	*Ictalurus punctatus*	Epidermal plasmoidia	USA
MG181225	*Henneguya santarenensis*	*Phractocephalus hemioliopterus*	Gills	Brazil
HQ655111	*Henneguya eirasi*	*Pseudoplatystoma fasciatum*	Gills	Brazil
MH300136	*Henneguya mystasi*	*Mystus vittatus*	Gills	India
KF296349	*Myxobolus pantanalis*	*Salminus brasiliensis*	Gills	Brazil
KP030760	*Henneguya* sp. 2 PBS-2015	*Auchenoglanis occidentalis*	Gills	Kenya

Table 3. *Myxospores* species > 88% identity, and query cover > 94% obtained from the GenBank and used for phylogenetic analysis of *H. qenasuprabranchiae* n. sp. described in the present study.

Accession No.	Species	Host origin	Infected organ	Locality
MT231731	*H. qenasuprabranchiae* n. sp	*C. gariepinus*	Extra respiratory organs	Egypt
KP990669	*Henneguya* sp. 1 HS-2015	*C. gariepinus*	Extra respiratory organs	Egypt
MT231729	*Henneguya* sp. Qena2	*C. gariepinus*	Stomach	Egypt
MK811030	*Henneguya* sp. y BZ-2019	*Ictalurus punctatus*	------	China
MZ905344	*Henneguya postexilis*	*Ictalurus punctatus*	Gills	USA
FJ468488	*Henneguya pellis*	*Ictalurus furcatus*	External/internal pseudocyst	USA
MZ905347	*Henneguya ictaluri*	*Dero digitata*	-----	USA
AF195510	*Henneguya ictaluri*	*Ictalurus punctatus*	Gills	USA
OP070162	*Henneguya* sp. br DHV-2022	*Rhamdia quelen*	Gills	Brazil
MG181225	*Henneguya santarenensis*	Amazonian pimelodid	Gills	Brazil
KF263537	*Helioactinomyxon* type 1 sp. TGR-2014	*Dero digitata*	Gills	USA
AF021878	*Aurantiactinomyxon mississippiensis*	*Dero digitata*	Gills	USA
MT231730	*Henneguya* sp. Qena3	*C. gariepinus*	Intestine	Egypt

3. Results

Visible myxosporean cyst infestations were observed in the gills and extra respiratory organs of 33 (27.5%) of the 120 *C. gariepinus* specimens examined. Myxosporean cysts (numbering 10–15/fish) were visible to the naked eye on the gills of 18 (15%) of the parasitized fish. The gill filaments of these infected fish displayed white, oval, cyst-like nodules, each measuring 1-2 mm in diameter. The consistency of the cysts was firm, and they contained myxospores in various phases of development (**Fig.1a**).

From the remaining *C. gariepinus* examined, 15 samples (12.5%) were infected with cysts in their extra respiratory organs (4–8 cysts/fish) that were visible to the naked eye. Infected fish had yellowish white plasmodia with globular or sub-globular raised cyst-like nodules on the extra respiratory organ wall measuring 3-5 mm in diameter and containing a milky, viscous fluid harboring developing myxospores **(Fig. 1b).**

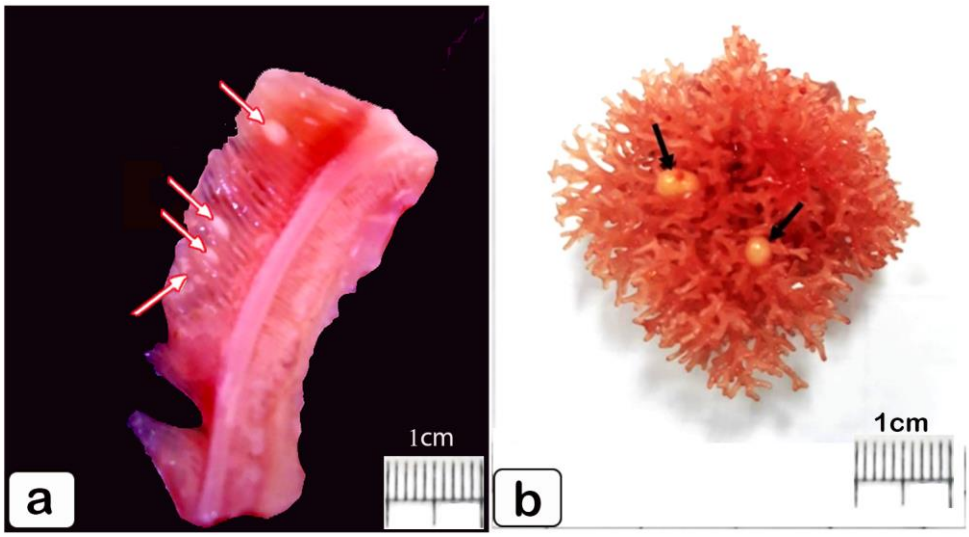

Fig. 1. Cyst-like nodules in *Clarias gariepinus.* (**a**) Gill lamellae (white arrow) infected with *H. qenabranchiae* n. sp. (**b**) Extra respiratory organ tissue (black arrows indicate cysts) infected with *H. qenasuprabranchiae* n. sp. Scale bars = 1cm.

Fresh, mature *Henneguya* sp. spores from the catfish gills were pyriform in the valvular view with a blunt anterior end **(Fig. 2a)**, while in the sutural view they appeared fusiform with a slightly visible suture line **(Fig. 2b).** The length of the spore body measured 14.2–15.87 (mean: 15.03) µm and the width was 3.9–4.17 (mean: 4.03) µm. Two ellipsoidal, equal polar capsules occupied nearly half of each spore, with 7-9 turns of polar tubules. Their lengths were 6.97–7.8 (mean: 7.43) µm and their widths were 1.9–1.7 (1.78) µm. The thread-like bifurcated caudal process was relatively long, measuring 37.3 -38.4 (mean: 37.8) µm. The sporoplasm contained a single spherical nucleus and no iodinophilous vacuole (**Figs. 3a, 3b, and 4a).** Scanning electron microscope images revealed that *Henneguya* sp. spores from the catfish gills had a pyriform spore body, smooth surface, and were gradually drawn out to form long, tapering caudal projections. **(Figs. 5a, 5b).**

The fresh, mature *Henneguya* sp. spores from catfish extrarespiratory organs were ovoid shaped in the valvular view with a protruding, rounded anterior end (**Fig. 2c),** while in the sutural view they appeared fusiform with a visible suture line **(Fig. 2d).** The length of the spore body was 12.2-14.5 (mean: 13.4) µm and the width was 4.5-5.3 (mean: 4.9) µm. Two polar capsules, elongated, unequal in length, blunt at the posterior end, that tapered anteriorly and occupied nearly half of the spore with 8-10 turns of polar tubules, were

present. Their length was 6.2–7.4 (mean: 6.8) µm in the large one and 5.3–6.1 (mean: 5.7) µm in the smaller polar capsule, and their widths were 1.5–2.3 (mean: 1.9) µm, whilst the extruded filaments measured 22–24 µm in length. Two equal caudal processes extending behind the spore measured 20.5-29.7 (mean: 25.4) µm. The sporoplasm contained rounded, central iodinophilous vacuoles **(Figs. 3c, 3d, and 4b).** The scanning electron microscope images of the *Henneguya* sp. spores from catfish extrarespiratory organs revealed a smooth, ovoid spore body with a slightly protruding anterior end that had a pore for the discharge of the polar filaments **(Figs. 5c, 5d).**

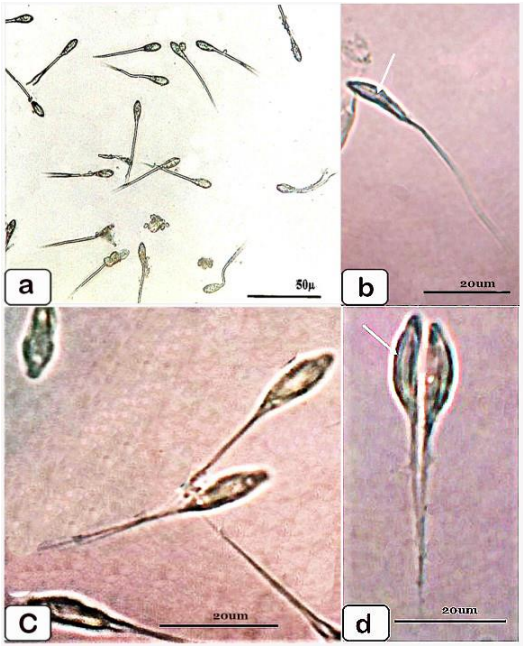

Fig. 2. Light photomicrographs of fresh, unstained, fixed mature myxospores. *H. qenabranchiae* n. sp. myxospores from the gills of *Clarias gariepinus* (**a**) valvular view, (**b**) sutural view showing the suture line (white arrow). *H. qenasuprabranchiae* n. sp. myxospores from the extra respiratory organs of *Clarias gariepinus*, (**c**) valvular view, and (**d**) sutural view showing the suture line (white arrow). Scale bars = a) 50 µm, b-d) 20 µm.

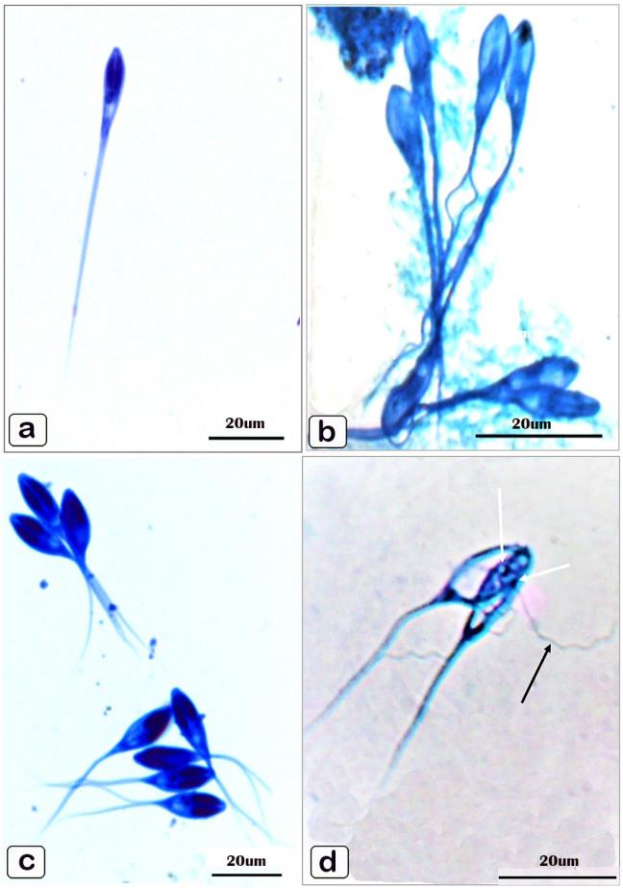

Fig. 3. Giemsa-stained mature myxospores. (**a,b**) *H. qenabranchiae* n. sp. myxospores with an equal polar capsule and unnucleated sporoplasm. (**c**) *H. qenasuprabranchiae* n. sp. myxospores with an ovoid body spore with an unequal polar capsule and circular vacuole, and (**d**) extruded polar filament (black arrow) and kinetoplast (white arrow). Scale bars = 20µm.

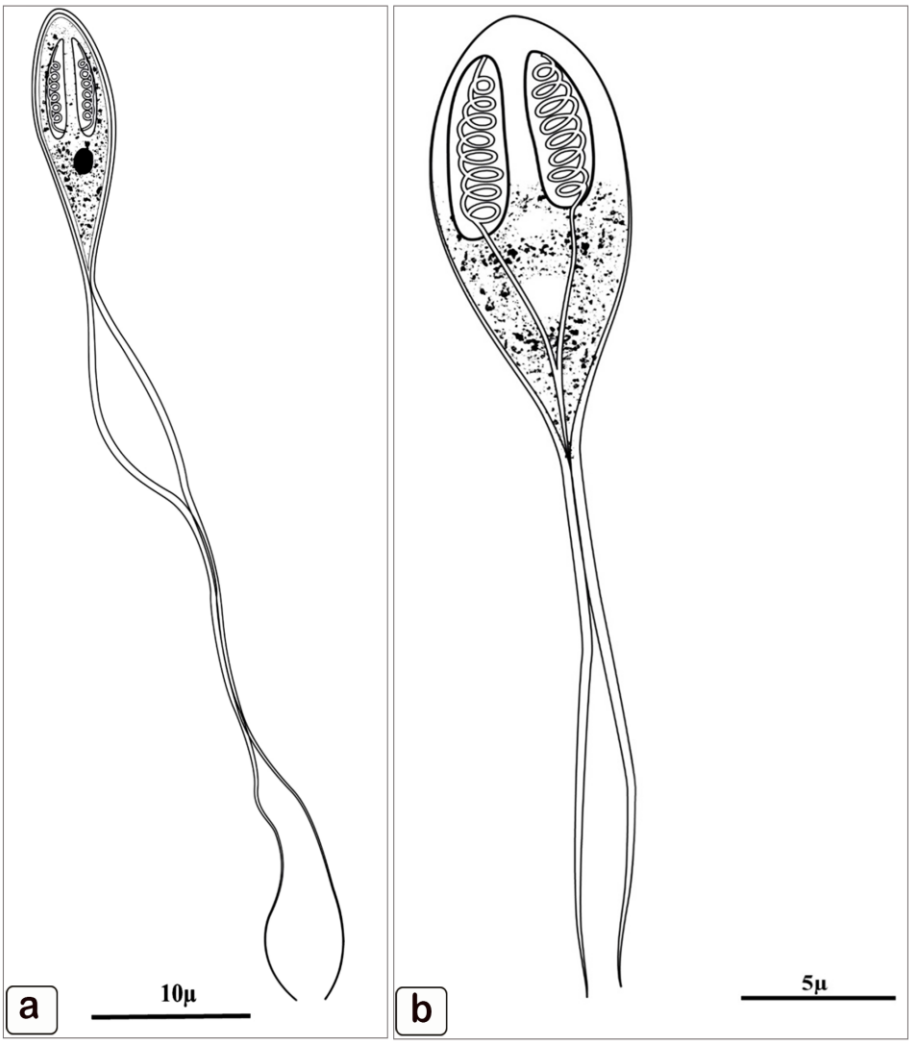

Fig. 4. Schematic drawing of mature myxospores extracted from *Clarias gariepinus*. (**a**) *H. qenabranchiae* n. sp. myxospore from the gills, (**b**) *H. qenasuprabranchiae* n. sp. myxospore from the extra respiratory organs. Scale bars = a) 10 µm, b) 5 µm.

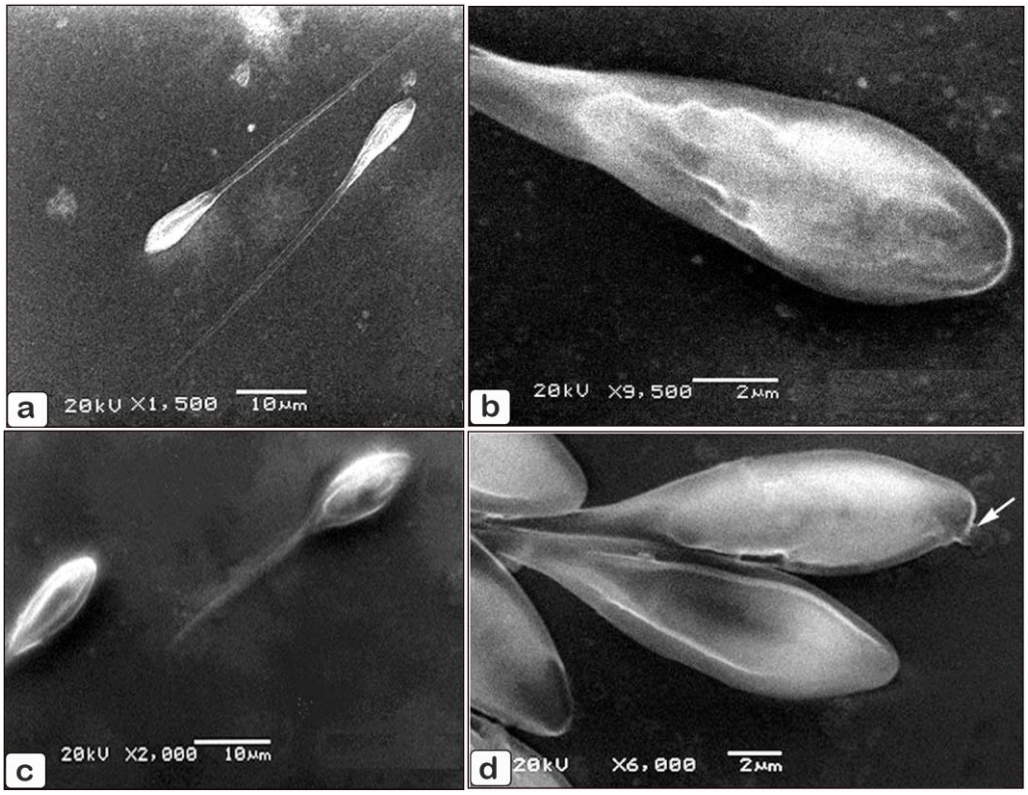

Fig. 5. Scanning electron micrograph of mature myxospores from *Clarias gariepinus*. (**a**) *H. qenabranchiae* n. sp. myxospores from the gills, and (**b**) its spore body, and (**c**) *H. qenasuprabranchiae* n. sp. myxospores from the extra respiratory organs, and (**d**) its spore body showing an anterior pore for discharge of polar filaments. Scale bars = a+c) 10 µm, b+d) 2 µm.

3.1 Taxonomic summary for the *Henneguya* sp. isolated from the gills

Name: *H. qenabranchiae* n. sp. (Myxosporea: Myxobolidae)

Host: Freshwater African sharptooth catfish, *C. gariepinus* (Burchell, 1822) (Siluriforme: Clariidae)

Site of infection: Gill filaments

Specimen deposit: Giemsa-stained myxospore slides and histological sections were given the accession numbers MYXO/1/140 and MYXO/1/230 and sent to the Fish Diseases Department, Faculty of Veterinary Medicine, South Valley University, Qena Province. This sample's 18S rDNA sequence was sent to GenBank (www.ncbi.nlm.nih.gov/genbank) with the accession number MT231728.

Locality: Nile River, Qena Province, Egypt (26° 10’ 12” N, 32° 43’ 38” E)

Etymology: The species was named after the locality where samples were collected (Qena) and the site of infection, the gills (branchiae).

Remarks: The morphometric comparison of *H. qenabranchiae* n. sp. and other *Henneguya* spp. presented in **Table 4** revealed similarities in spore body and polar capsule dimensions with *Henneguya* sp. (Saleh, 2015). Some key similarities and differences were its caudal appendage was shorter than present in *Henneguya* sp.,

whereas *H. postexilis* (Woodyard et al., 2022) and *H. suprabranchiae* (Abdel-Baki et al., 2011) have similar lengths for both spore body and caudal appendage, but they have unequal polar capsules. In addition although *H. samochimensis* (Reed et al., 2003) has a similar caudal appendage length it has slightly different dimensions of the other structures. *H. qenabranchiae* n. sp. was also characterized morphologically as containing a small amount of sporoplasm containing a spherical nucleus and a long, thin, bifurcated caudal appendage.

The host specificity, locality, and location of plasmodia in the host should also been considered, therfore it is worth mentioning that *Henneguya* sp. 1 (Saleh, 2015), *H. branchialis* (Ashmawy et al., 1989), and *H. suprabranchiae* (Morsy et al., 2012) infect the extra respiratory organs, gills, and extra-respiratory organs, respectively, of *C. gariepinus* in Egypt. Accordingly, based on light and electron microscopic investigations, the detected myxosporean parasites in the gills were identified as species of the genus *Henneguya* and named *H. qenabranchiae* n. sp. **Table 4** shows comparative descriptions of *H. qenabranchiae* n. sp. against other *Henneguya* species.

Table 4. Comparative data of *H. qenabranchiae* n. sp. with previously described *Henneguya* spp. parasites. All measurements are given as range (mean) and n=25.

Parasite species	*H. qenabranchiae* n. sp.	***Henneguya* sp. 1 (Saleh, 2015)**	***H. postexilis* (Woodyard et al., 2022)**	***H. samochimensis* (Reed et al., 2003)**	***H. branchialis* (Ashmawy et al., 1989)**	***H. suprabranchiae* (Morsy et al., 2012)**	***H. suprabranchiae* (Abdel-Baki et al., 2011)**
Host	*C. gariepinus*	*C. gariepinus*	*Ictalurus punctatus*	*C. gariepinus*	*C. gariepinus*	*C. gariepinus*	*C. gariepinus*
Infection site	Gills	Extra respiratory organs	Gills	Gills	Gills	Extra respiratory organs	Gills
Spore morphology	Spore body pyriform, sporoplasm has nucleus, equal polar capsule, Long narrow forked tail.	Spore body ovoid, anterior end of spore is pointed.	Spore body lanceolate, Polar capsules are pyriform, unequal in length. Caudal processes bifurcated.	Mature spore body elongated to oval with bluntly pointed narrow anterior end. Two pyriform polar capsules. Caudal appendages separated from each other.	-----	Spore body ovoid.	Spore body oval, binuleated sporoplasm. Forked tail.
Spore body length (µm)	14.2-15.87 (15.03)	15.99±0.3 (15.7-16.2)	12.1-17.2 (15.5)	12.3-15.0 (13.7)	13.3-15.4 (14.5)	11-14	12.1-15.7 (14.3±0.7)
Spore body width (µm)	3.9-4.17 (4.03)	4.91±0.7 (4.2-5.6)	3.6-4.8 (4.1±0.3)	5.0-7.0 (6.0)	4.7-5.6 (5.6)	2-5	4.9-7 (6.0±0.5)
Polar capsule length (µm)	6.97-7.8 (7.43)	6.48±0.2 (6.3-6.7)	4.4-6.7 (5.9±0.6) 4.4-6.4 (5.6±0.5)	5.0-6.0 (5.6)	5.5-7.7 (6.2)	2.5-5.0	5.7-7.1 (6.4±0.4)
Polar capsule width (µm)	1.9-1.7 (1.78)	1.75±0.2 (1.5-1.9)	1.1-1.6 (1.4±0.1)	1.3-1.9 (1.9)	2.1-2.5 (2.2)	1.5-4	2.1-2.8 (2.3±0.2)
Coils	7-9	-----	6-8	8	-----	-----	8-9
Caudal projection length (µm)	37.3-38.4 (37.8)	21.18±0.9 (20.3-22)	25.7-38.1 (31.2±4.6)	34.7-35.3 (36.6)	14.6-25.8 (17.3)	27-30	28.5-41.4 (35.1±3.1)
Total length (µm)	51.8-53.3 (52.5)	-----	42.7-49.1 (45.9±2.2)	47.0-53.0 (50.3)	27.9-41.2	-----	42.8-56.4 (49.9±3.3)

3.2. Taxonomic summary for Henneguya sp. isolated from the extra respiratory organ

Name: *H. qenasuprabranchiae* n. sp. (Myxosporea: Myxobolidae)

Host: Freshwater African sharptooth catfish, *C. gariepinus* (Burchell, 1822) (Siluriforme: Clariidae)

Site of infection: Extra respiratory organs

Specimen deposit: Geimsa-stained myxospore slides and histological sections were deposited at the Fish Diseases Department, Faculty of Veterinary Medicine, South Valley University, Qena Province with accession numbers MYXO/1/141 and MYXO/1/231, respectively. The 18S rDNA sequence obtained from this sample was submitted to GenBank (www.ncbi.nlm.nih.gov/genbank) under accession number MT231731.

Locality: River Nile, Qena Province, Egypt (26° 10’ 12" N, 32° 43’ 38" E)

Etymology: The species was named after the locality where samples were collected (Qena) and the site of infection, the extra respiratory organ (suprabranchiae).

Remarks: Morphometric and morphological comparisons showed that there was a close similarity with *Henneguya* sp.1 (Saleh, 2015), *H. suprabranchiae* (El-Mansy, 2002; El-Mansy & Bashtar, 2002; Morsy et al., 2012), and *H. branchialis* (Ashmawy et al., 1989), which all infect the same host, *C. gariepinus,* in Egypt. However, the present *Henneguya* showed unequal polar capsules in most of the spores, in contrast to the other species. Whilst *H. postexilis* (Woodyard et al., 2022) and *H. pellis* (Griffin et al., 2009) showed some similarities with regards to morphological and dimensional comparisons, they have different hosts, localities, and infection sites to the present *Henneguya*. Accordingly, based on light and electron microscopic investigations, the detected myxosporean parasites in the extra respiratory organs were identified as species of the genus *Henneguya* and named *H. qenasuprabranchiae* n. sp. **Table 5** contains comparative descriptions of *H. qenasuprabranchiae* n. sp against other *Henneguya* spp.

Table 5. Comparative data of *H. qenasuprabranchiae* n. sp. with previously described *Henneguya* spp. parasites. All measurements are given as range (mean) and n = 25.

Parasite species	*H. qenasuprabranchiae* n. sp.	***H. suprabranchiae* (Landsberg, 1987)**	***Henneguya* sp. 1 (Saleh, 2015)**	***H. postexilis* (Woodyard et al., 2022)**	***H. branchialis* (Ashmawy et al., 1989)**	***H. pellis* (Griffin et al., 2009)**	***H. suprabranchiae* (Morsy et al., 2012)**	***H. suprabranchiae* (El-Mansy & Bashtar, 2002)**	***H. suprabranchiae* (El-Mansy, 2002)**
Host	*C. gariepinus*	*C. gariepinus*	*C. gariepinus*	*Ictalurus punctatus*	*C. gariepinus*	*Ictalurus furcatus*	*C. gariepinus*	*C. gariepinus*	*C. gariepinus*
Infection site	Extra-respiratory organs	Extra-respiratory organs	Extra-respiratory organs	Gills	Gills	External & internal pseudocyst	Extra-respiratory organs	Extra-respiratory organs	Intestine
Spore morphology	Ovoid shape fusiform body. Unequal polar capsules, forked tail.	Larger polar capsules, divided caudal processes at tip.	Spore body ovoid. Anterior end of spore pointed.	Spore body lanceolate. Polar capsules pyriform, unequal in length. Caudal processes bifurcated.	-------	Lanceolate myxospores, flattened parallel to the suture line. Unequal pyriform polar capsules.	Spore body ovoid.	Elongated fusiform body. Two thin caudal processes.	Mature spores elongated with a rounded, anterior end. Two thin and equal caudal processes. Rounded central, iodinophilous vacuole.
Spore body length (µm)	12.2-14.5 (13.4)	12.2-14.3 (13.5)	15.99±0.3 (15.7-16.2)	12.1-17.2 (15.5)	13.3-15.4 (14.5)	13.0-17.1 (14.8±1.1)	11-14	12-14	12.1-12.7 (12.4)
Spore body width (µm)	4.5-5.3 (4.9)	5.6-6.9 (6.4)	4.91±0.7 (4.2-5.6)	3.6-4.8 (4.1±0.3)	4.7-5.6 (5.6)	4.0-7.4 (4.8±0.8)	2-5	5.5-6.7	4.5-6.0 (5.3)
Polar capsule length (µm)	L: 6.2-7.4(6.8) S: 5.3-6.1(5.7)	7.0-8.1 (7.6)	6.48±0.2 (6.3-6.7)	4.4-6.7 (5.9±0.6) 4.4-6.4 (5.6±0.5)	5.5-7.7 (6.2)	6.2-8.4 (7.2±0.6) 5.5-8.0 (6.5±0.5)	2.5-5.0	6.5-7.8	5.3-6.0 (5.7)
Polar capsule width (µm)	1.5-2.3 (1.9)	1.8-2.3 (2.1)	1.75±0.2 (1.5-1.9)	1.1-1.6 (1.4±0.1)	2.1-2.5 (2.2)	1.4-1.9 (1.7±0.2)	1.5-4	1.9-2.0	1.1-1.5 (1.3)
Coils	8-10	-----	-----	6-8	-----	8	-----	-----	8-12
Caudal projection length (µm)	20.5-29.7 (25.4)	18.5-29.0 (24.0)	21.18±0.9 (20.3-22)	25.7-38.1 (31.2±4.6)	14.6-25.8 (17.3)	57.4-96.4 (77.7±8.8)	27-30	19-28.9	22.9-24.4 (23.7)
Total length (µm)	33.4-44.2 (38.87)	30.7-43.3 (37.5)	-----	42.7-49.1 (45.9±2.2)	27.9-41.2	73.3-113.5 (92.5±9.2)	-----	38.4-43.0	-----

3.3. Histopathological results

Gross anatomical investigations showed that uninfected fish gills had a normal appearance in terms of color, shape, and consistency. In contrast, infected gills had a large nodular mass at the end of the gill filaments, which resulted in thickening and adhesion of the attached lamellae covered with mucoid exudate. There was also sloughing and desquamation of the gill lamellae tips, resulting in pale or grayish colored necrotic areas. Otherwise, areas of the gill arches appeared very dark red in color as a result of congestion and stagnation of the blood vessels.

Cross sectional histopathological screening showed that uninfected fish had normal histological architecture with a symmetrical arrangement of the gill filaments, which included the gill lamella, filament epithelium, and central venous sinus **(Figs. 6a, 6b).** In contrast, the infected fish showed large plasmodia consisting of presporogenic and mature myxospores surrounded by a thick eosinophilic wall, which was implanted at the tips of gill filaments (**Figs. 7a, 7b).** Besides this, developmental trophozoite, sporocyst, and gamont stages embedded within the gill tissues were revealed **(Figs. 7c, 7d).**

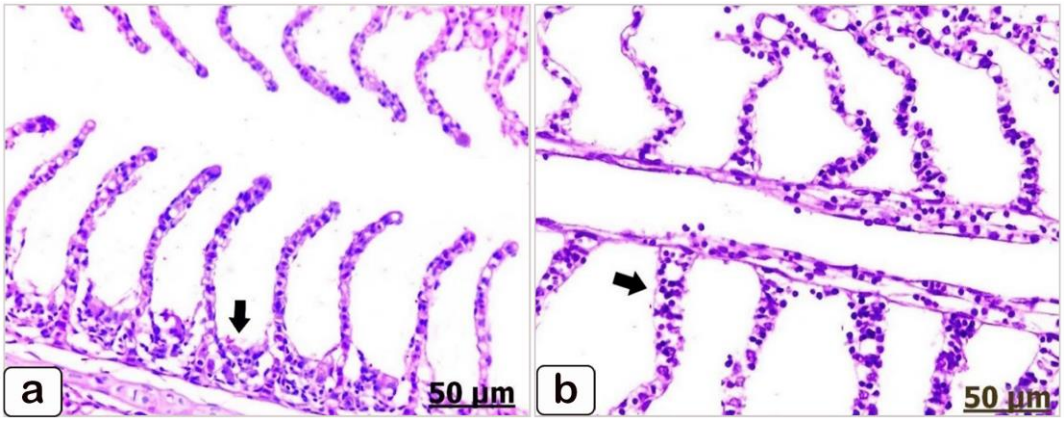

Fig. 6. Photomicrographs of H&E stained control (non-infected) *C. gariepinus* gills. (**a**) Appropriately coordinated primary lamellae (filament epithelium is indicated by black arrows), and (**b**) symmetrical secondary lamellae (black arrow). Scale bars = 50 µm.

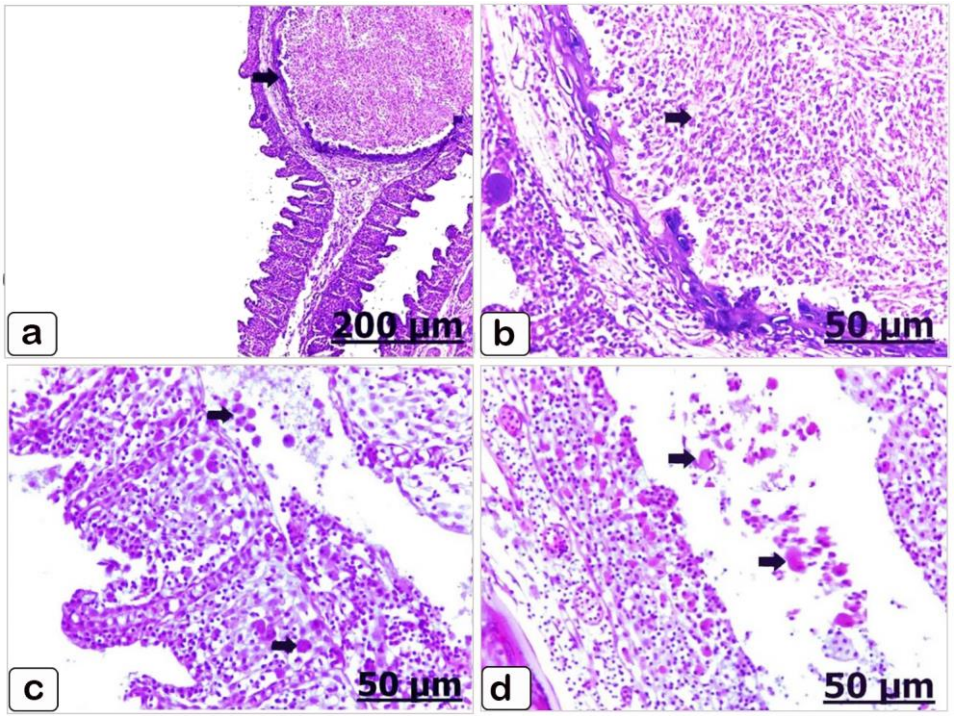

Fig. 7. Photomicrographs of H&E stained infected *C. gariepinus* gills. (**a**) Large plasmodia (black arrow) consisting of presporogenic and mature myxospores surrounded with a thick eosinophilic wall and implanted at tips of gills filaments. (**b**) High power of panel a showing large thick myxospores walled plasmodium (black arrow). (**c, d**) Detection of developing stages of *Henneguya* involving trophozoite, sporocyst, and gamont embedded within gills tissues (black arrows). Scale bars = a) 200 µm, b-c) 50 µm.

Histological changes in the gill lamellae associated with *Henneguya* plasmodia included hyperplasia of the epithelial lining primary lamellae, as well as thickening and dilatation of the central venous sinus **(Figs. 8 a, 8b)**, which resulted in partial adhesion and fusion of the secondary lamellae with hyperactivity of ionocytes (chloride cells), as well as shortening and dwarfism on the opposite side **(Fig. 8c)**. Curling of secondary lamellae **(Fig. 8d)** and necrosis with sloughing and desquamation of epithelial lining lamellae were also observed **(Fig. 8e)**; besides this, a focal area of inflammatory cells replaced the necrotic lamellae **(Fig. 8f)**. The gill arches also exhibited severe congestion and dilatation of the blood vessels with stagnant RBCs **(Figs. 9a, 9b)**. Additionally, dilatation and thickening of the walls of the blood vessels with leucocytic cell infiltration and fibrous tissues were noticed **(Fig. 9c)**. Ultimately, there was swelling and hypertrophy of the chondrocytes, in addition to intense infiltration of inflammatory cells **(Fig. 9d).**

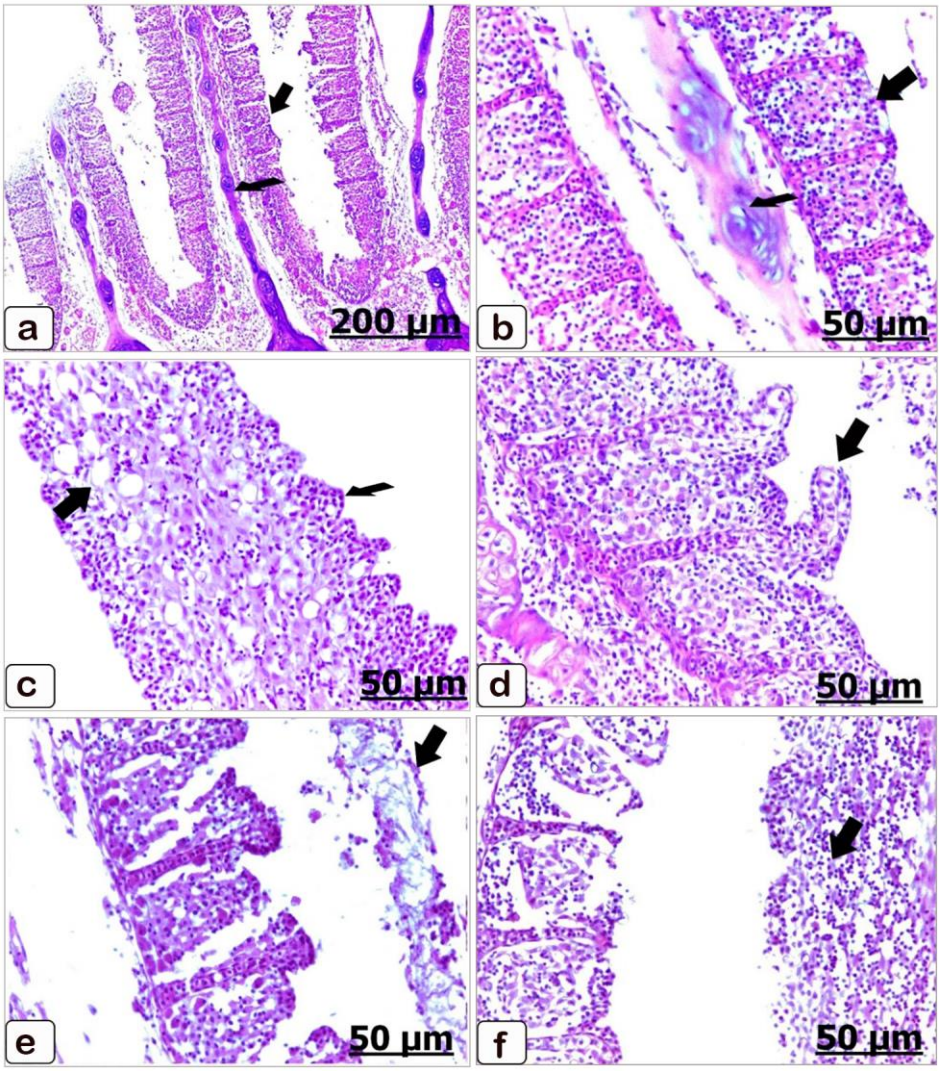

Fig. 8. Photomicrographs of H&E stained infected *C. gariepinus* gill filaments. (**a**) Hyperplasia of the epithelial lining primary lamellae (thick arrow), as well thickening and dilatation of the central venous sinus (thin arrow). (**b**) High power of panel a showing hyperplasia with increased cellularity of the epithelial lining primary lamellae (thick arrow), in addition to thickening and dilatation of the central venous sinus (thin arrow); (**c**) leading to partial adhesion and fusion of the secondary lamellae with hyperactivity of ionocytes (chloride cells; thick arrow), with shortening on the opposite side (thin arrow); (**d**) in addition to curling of secondary lamellae; (**e**) necrosis of the gill lamellae with desquamation and sloughing of the epithelial lining (black arrow); (**f**) and subsequently an intensive degree of inflammatory cell infiltration replacing necrotic areas (black arrow). Scale bars = a) 200 µm and c-f) 50 µm.

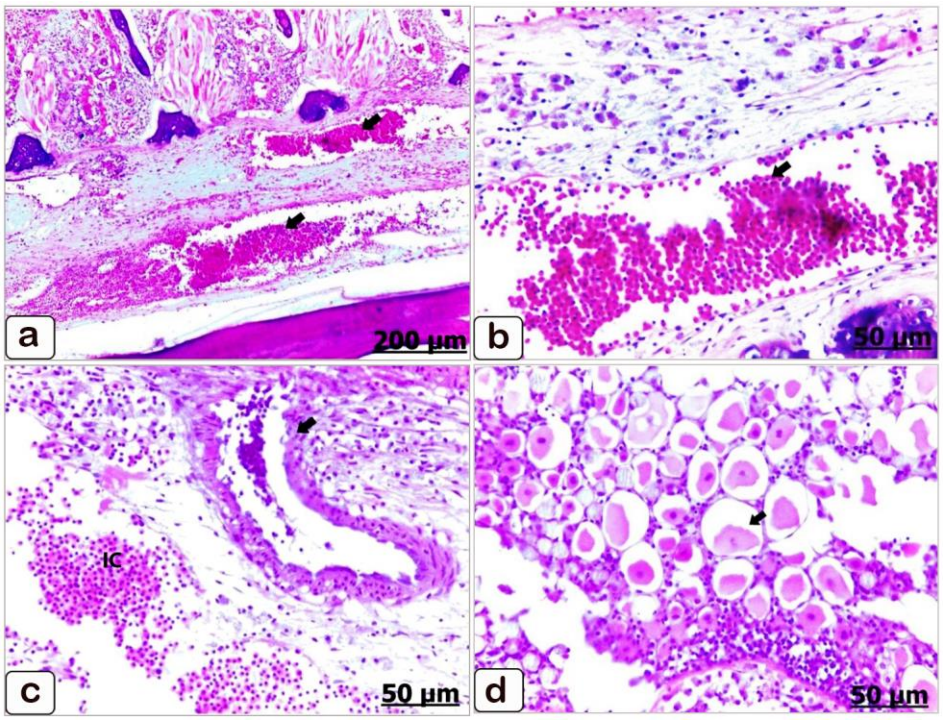

Fig. 9. Photomicrographs of H&E stained infected *C. gariepinus* gill arch showing dilation, congestion and hypertrophic chondrocytes. (a) Exhibiting severe dilatation and congestion of the blood vessels with stagnant red blood cells (RBCs; black arrow). (**b**) High power of panel a showing dilated and congested blood vessels with stagnant RBCs (black arrow). (**c**) Dilatation and thickening of the blood vessel wall (black arrow) with inflammatory cells (IC) and fibrous tissues, (**c**) and subsequently swollen and hypertrophic chondrocytes (black arrow). Scale bars = a) 200 µm and b-d) 50 µm.

In the extra respiratory organs of uninfected fish, the gross appearance of the dendritic tissues seemed to be normal in terms of consistency and texture. Infected fish, on the other hand, showed grayish, pinpoint patches of necrosis scattered throughout the tissues. Control, non-infected fish displayed normal architecture within the dendritic tissues, which were composed of epithelium, connective tissue, elastic cartilage, perichondrium, connective tissue septa, blood vessels, and chondrocytes **(Figs. 10a, 10b)**. Regarding the extra respiratory organs of the infected fish, variable sized myxospores that formed plasmodia were present, and there was also remarkable infiltration of inflammatory cells **(Fig. 10a, 10b)**. Furthermore, larval stages in *Henneguya* cysts were surrounded by a fibrous wall, as well as a focal accumulation of inflammatory cell infiltration **(Fig. 11)**.

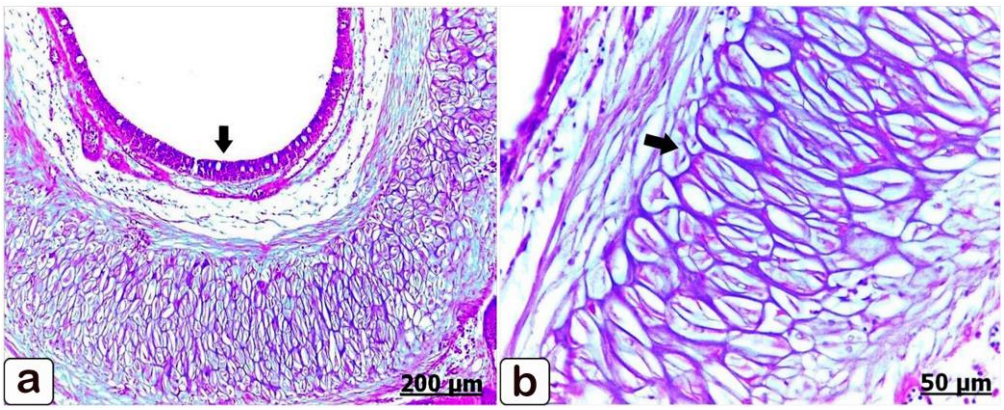

Fig. 10. Photomicrographs of H&E stained control (non-infected) *C. gariepinus* extra respiratory organ tissue. (**a**) Intact dendritic tissues (black arrow) with normal epithelial lining. (**b**) Typical arrangement of chondrocytes, appropriately ordered (black arrow). Scale bars = a) 200 µm & b) 50 µm.

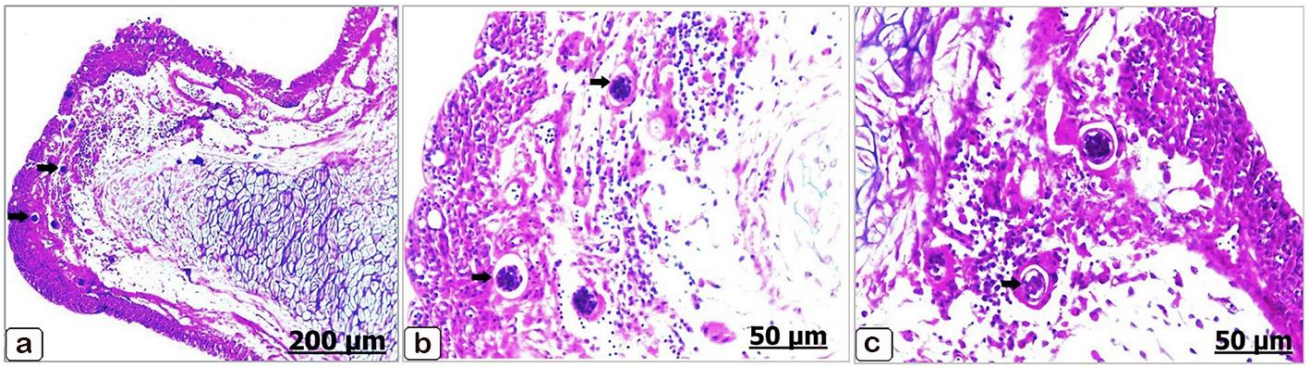

Fig. 11. Photomicrographs of H&E stained infected *C. gariepinus* extra respiratory organs exhibiting myxospores and cysts. (**a**) Variable-sized spores formed plasmodia filled with myxozoan spores (black arrows). (**b**) High power of panel a showing myxospores formed plasmodia in addition to prominent infiltration of inflammatory cells (black arrows). (**c**) *Henneguya* cyst containing larva stage surrounded with a fibrous wall, as well as focal aggregation of inflammatory cells infiltration (black arrow). Scale bars = a) 200 µm and b-c) 50 µm).

The characteristic features of the histopathological aspects in relation to the presence of a *Henneguya* cyst were hyperplasia of the epithelial lining and hyperplasia of the goblet cells **(Figs. 12a, 12b)**. Severe necrosis with atrophied chondrocytes replaced by inflammatory cell infiltration was also distinctive **(Figs. 12c, 12d)**. The blood vessels exhibited severe dilatation and congestion and notable engorgement with RBCs **(Fig. 12e)**. Furthermore, severe thickening of the blood vessel wall with fibrous tissues and inflammatory cells was distinguished **(Fig. 12f)**.

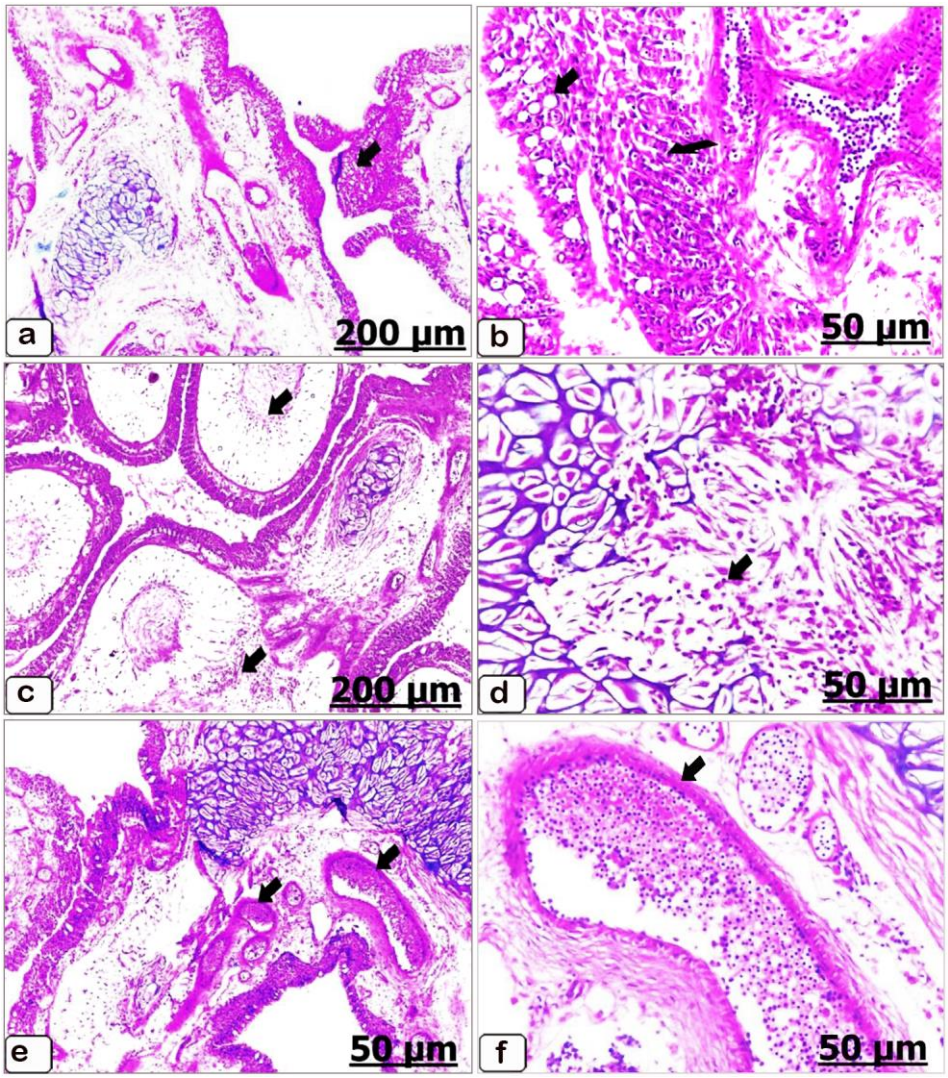

Fig. 12. Photomicrographs of H&E stained infected *C. gariepinus* extra respiratory organs showing hyperplasia, necrosis, dilation and congestion. (**a**) Hyperplasia of the epithelial lining (long arrow) with hyperplasia of the goblet cells (short arrow). (**b)** High power of panel a showing hyperplasia of the epithelial lining with hyperplastic goblet cells, (**c**) severe necrosis with atrophied chondrocytes (black arrows), (**d**) high power of panel c showing necrosis of the chondrocytes replaced by focal aggregation of inflammatory cells infiltration (black arrow). (**e**) Severe dilatation and congestion of the blood vessels due to engorgement with red blood cells (RBCs; black arrows), (**f**) high power of panel e showing severe dilatation and congestion of the blood vessels with stagnant RBCs, as well thickening to blood vessels wall (black arrow) with fibrous tissues and inflammatory cells infiltration. Scale bars = a+c) 200 µm & b+d-f) 50 µm.

3.4. Molecular identification

Sequencing of small subunit (SSU) rDNA from *H. qenabranchiae* n. sp. spores resulted in a 427 bp sequence that revealed various percentages of similarity with different *Henneguya* spp. sequences available in GenBank. The greatest similarity with 100% query cover was between the *Henneguya* sp. 1 HS-2015 strain (accession number KP990669) and *Henneguya* sp. Qena 4 (*H. qenasuprabranchiae* n. sp.) from the present study (accession number MT231731), which revealed 99.53% and 99.30% sequence identity, respectively.

Molecular analyses of the SSU 18S rDNA isolated from *H. qenasuprabranchiae* n. sp. spores amplified 887 nucleotides, and BLASTn searches obtained various percentages of similarity with different *Henneguya* spp. sequences available in GenBank. The greatest similarity was with the *Henneguya* sp. 1HS-2015 strain (accession number KP990669), which revealed 99.64% sequence identity with query cover of 94%; *Henneguya* sp. Qena 2 (accession number MT231729), with 92.74% sequence identity, and query cover of 94%; *Henneguya* sp. BZ-2019 (accession number MK811030); and *H. postexilis* (accession number MZ905344), both with 88.59% sequence identity and a query cover of 98%.

3.5. Phylogenetic analysis

Phylogenetic analysis of the parasite 18S rDNA sequences, using the maximum likelihood method, against myxozoan sequences deposited in GenBank revealed clustering of each of the *H. qenabranchiae* n. sp. and *H. qenasuprabranchiae* n. sp. with the closest myxozoan isolates in distinct lineages. *H. qenabranchiae* n. sp. infected the gills and is part of a weakly supported subclade that includes parasites of various organ types. These include *Henneguya* sp. in the extra respiratory organs found in the present study and another *Henneguya* sp. that infects the same host (*C. gariepinus*, of the family Clariidae in Egypt) **(Fig. 13)**. Conversely, *H. qenasuprabranchiae* n. sp. clustered in a well-supported subclade composed of *Henneguya* sp. that infect the extra respiratory organs of *C. gariepinus*, within family Clariidae, in Egypt **(Fig. 14)**.

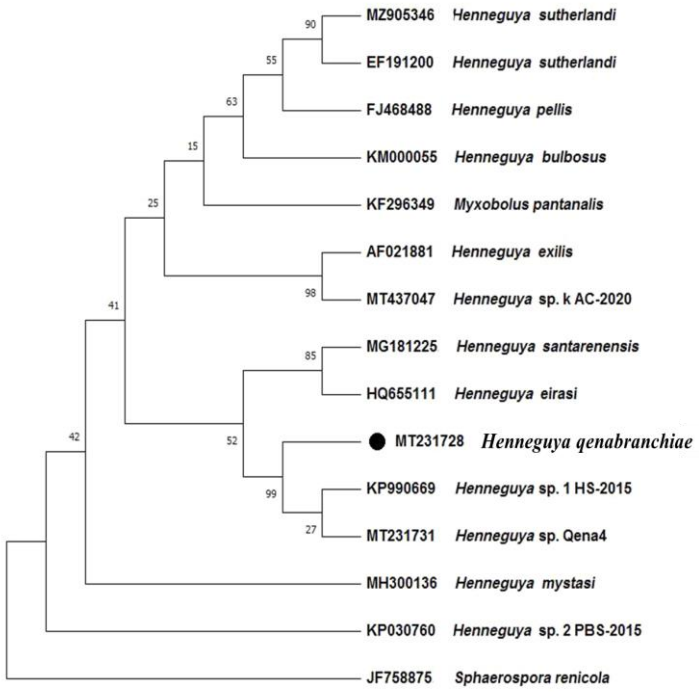

Fig. 13. Maximum likelihood phylogenetic tree showing the relationship between *H. qenabranchiae* n. sp. described in this study and the closest myxozoan sequences from GenBank based on small subunit ribosomal DNA (SSU-rDNA). *Sphaerospora renicola* was used as the outgroup. Numbers at branching points indicate bootstrapping confidence levels from maximum likelihood. GenBank accession numbers are listed beside the species name. The black circle represents the species described in the present study.

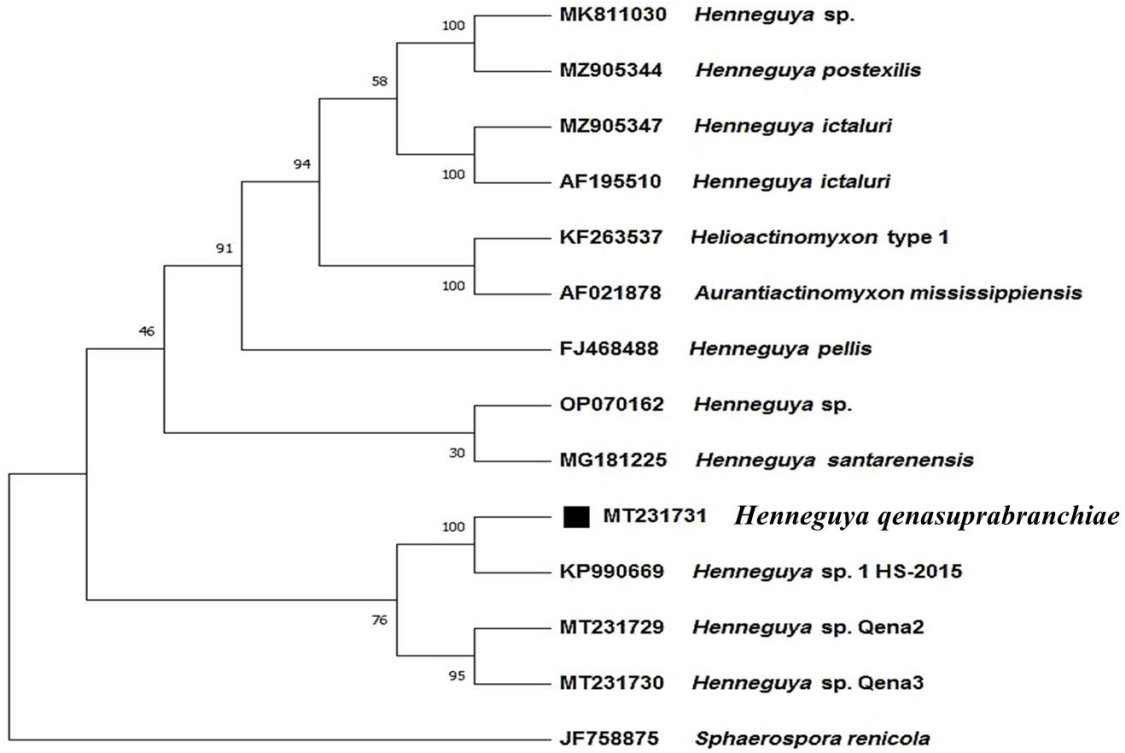

Fig. 14. Maximum likelihood phylogenetic tree showing the relationship between *H. qenasuprabranchiae* n. sp. described in this study and the closest myxozoan sequences obtained from GenBank based on small subunit ribosomal DNA (SSU-rDNA). *Sphaerospora renicola* was used as the outgroup. Numbers at the branching points indicate bootstrapping confidence levels from maximum likelihood. GenBank accession numbers are listed following the species name. The black square represents the species described in the present study.

4. Discussion

In this study, we identified a high prevalence of myxospores isolated from catfish respiratory organs, the catfish were located in the Nile River in the Qena Province. The cysts observed in the gills and extra respiratory organs from the infected *C. gariepinus* were consistent with those reported in previous studies (Abdel-Ghaffar et al., 1995; Ashmawy et al., 1989; Diab et al., 2006; Eissa et al., 2002; Emeish, 2006; Endrawes, 2001; Marwan et al., 1998; Osman, 2001; Saleh, 2015).

A number of different techniques were used to examine the *Henneguya* spp. discovered in the catfish. Morphometric comparison of the present *H. qenabranchiae* n. sp. spores against others showed similarities with *Henneguya* sp. 1 (Saleh, 2015) which infects the extra respiratory organs of *C. gariepinus*; *H. postexilis* (Woodyard et al., 2022) which infects the gills of *Ictalurus punctatus* in the USA; and *H. samochimensis* (Reed et al., 2003) which infects the gills of *C. gariepinus* in Botswana. In contrast, the morphological comparisons showed there was no obvious similarity between *H. qenabranchiae* n. sp., and the previously recorded species. Meanwhile morphometric comparisons of the spores from *H. qenasuprabranchiae* n. sp., against other known species showed similarities with *Henneguya* sp.1 (Saleh, 2015), *H. suprabranchiae* (El-Mansy, 2002; El-Mansy &Bashtar, 2002; Morsy et al., 2012) which infects different sites in *C. gariepinus* Egypt, and *H. branchialis* (Ashmawy et al., 1989) which infects both the gills and internal organs of the same host in Egypt. Morphological comparisons revealed significant similarities between the current *H. qenasuprabranchiae* n. sp., and *H. suprabranchiae* in terms of both site of infection (respiratory organs), host, and graphical locality. Morphometric and morphologic analyses of the present *Henneguya* spp., also indicated limited but significant differences between these similar species.

The scanning electron microscopy investigations showed that the two *Henneguya* spp. described in the present study both had smooth surfaces, as previously described for *H. voronini* n. sp. (Borkhanuddin et al., 2020), *H. aegea* (Katharios et al., 2020) and *Henneguya* spp. 1 and 2 (Emeish et al., 2022). The body shape of the present two species differed from that of *H. voronini* (Borkhanuddin et al., 2020), and *H. aegea* (Katharios et al., 2020), where the body is more elongated. The body shape of the present species, *H. qenabranchiae* n. sp., was more elongated than that of *H. qenasuprabranchiae* n. sp. and was similar to *Henneguya* sp. 1 (Emeish et al., 2022). The caudal projection in the present species *H. qenabranchiae* n. sp. was as long as *H. voronini* (Borkhanuddin et al., 2020), but the caudal projection in the present species *H. qenasuprabranchiae* n. sp. was shorter. The present species, *H. qenasuprabranchiae* n. sp. also had a short caudal projection, as previously observed in *Henneguya* sp. 2 (Emeish et al., 2022).

It is known that *Henneguya* spp. infect different tissues and hosts (Abdel-Ghaffar et al., 2008), causing serious damage attributed to the direct reaction of host tissues toward the parasites (Eissa et al., 2006). Histopathological examination demonstrated the presence of the spores in cross sections where henneguyosis affects gill-induced hyperplasia and fusion of gill lamellae, besides this, necrosis and congestion of the blood vessels were observed. Myxosporea infections are caused by pathogenic species that instigate physical and lethal damage to the gills and extra respiratory organs of the host (El-Matbouli et al., 1992; Sabri et al., 2010). In the gills, *Henneguya* induced difficulties in osmoregulation and respiration result from decreased oxygen uptake, which causes hypoxia (Lebelo et al., 2001) and much destructive damage to the tissues (El-Mansy, 2002). The extent of damage depends on the species of parasite and its life cycle stage, the intensity of infection, the host reaction, and its immune status (Lom & Dykova, 1995).

Regarding the extra respiratory organs, current data indicate the presence of chondrocyte necrosis with inflammatory cell exudation. Extra respiratory organs are used when the oxygen concentration in water is insufficient for gill respiration (Grizzle & Rogers, 1976). However, persistent plasmodium mass growth was linked to pressure atrophy on host chondrocytes, resulting in severe atrophy as well as damage to the endothelial lining of the hyaline cartilage. Likewise, the blood vessels were dilated and congested, particularly when plasmodia developed in size (El-Mansy & Bashtar, 2002). These factors were all observed in the present study.

Morphological similarities in *Henneguya* spp. make their identification and differentiation difficult. Molecular biology techniques have enabled the development of taxonomic studies (Adriano et al., 2009). When compared to the *Henneguya* spp. available at the NCBI, the sequence of *H. qenabranchiae* n. sp. identified in this study demonstrated 99.53% identity with the *Henneguya* sp.1 HS-2015 strain (accession number KP990669), infecting the same host in the same environment (Saleh, 2015). However, the morphologic and morphometric descriptions concluded that there were no distinct similarities between them. *H. qenasuprabranchiae* n. sp. showed considerable morphological similarities with *H. suprabranchiae* (accession number JN201199), however, these morphological similarities were not well supported by molecular data. The BLASTn results between them revealed identity in 99.7% of the cases and only query coverage of 37%. Therefore, it is difficult to prove that they are the same. In the Myxosporea, although interspecific variation in the SSU is typically >2 % (Fiala, 2006), within other Myxosporea genera, e.g., Myxobolus, interspecific differences in the SSU can be as low as 0.2% (Ferguson et al., 2008). Typically, **i**ntraspecific differences in SSU range from 0–3.6 % (Ferguson et al., 2008).

Phylogenetic analysis of the SSU rDNA of the studied *Henneguya* spp., as well as many other Myxosporea available in GenBank, the majority of which were *Henneguya*, found that they were indeed Myxobolidae of the genus *Henneguya*, infecting mainly Siluriformes fish, and confirmed their taxonomic position. Our study further confirms the findings of Fiala et al. (2015), with an intermingling of one *Myxobolus* sp. with *Henneguya* spp. in a separate subclade during phylogeny analysis of *H. qenabranchiae* n. sp. and intermingling of two other Myxosporea spp., *Helioactinomyxon* type 1 and *Aurantiactinomyxon mississippiensis* during phylogeny analysis of *H. qenasuprabranchiae* n. sp. Therefore, these findings do not support a phylogenetic separation between *Henneguya* spp. and other closely related genera, despite their morphological differences (Chen et al., 2020).

In the present study, a phylogenetic tree demonstrated that *Henneguya* spp. tend to form clades based on their geographical locality and family of the host fishes. As reported in prior studies, all parasites of hosts from the same family were clustered together (Ferguson et al., 2008; Naldoni et al., 2011). These results enable us to hypothesize that the ancestors of current hosts were infected by the ancestors of current parasites (Adriano et al., 2012). Previous studies (Burger et al., 2006; Fiala, 2006) also noted the importance of tissue specificity in Myxozoan evolution. The *H. qenasuprabranchiae* n. sp. phylogenetic tree in the present study confirms this, as it clustered in a well-supported subclade with the *Henneguya* sp. 1 HS-2015 strain (accession number KP990669) and both infected the same tissue type. Moreover, it shared a distinct subclade with our previously published work (Emeish et al., 2022) relating to two *Henneguya* spp. infecting the internal organs.

Analyses of the 18S SSU rDNA sequence of the *Henneguya* spp. indicate limited, but significant, genetic similarities, and as recorded by other researchers (Salim & Desser, 2000), taxonomic classification results agreed with traditional taxonomic classification using host records and tissue predilection. This supports the validity of these methods for classification purposes and the use of site, tissue, and host specificity as valid taxonomic characteristics to be considered alongside morphological traits in identifying myxospores as species.

5. Conclusions

This study describes two myxosporean species affecting the African sharptooth catfish (*C. gariepinus*) in the River Nile, Qena, Egypt. Morphological and molecular data indicate they are new species, nominated as *H. qenabranchiae* n. sp. and *H. qenasuprabranchiae* n. sp., which were isolated from the gills and extra respiratory organs, respectively. This study expands our knowledge and understanding of myxosporean parasite relationships in *C. gariepinus*, an economically important Clariidae fish species in Egypt.

Declarations

Informed Consent Statement: "Not applicable."

Ethics approval*:* The present study follows the ethical guidelines determined by animal experiment and research of South Valley University (RCOE-SVU- South Valley University) and was approved by the Ethical Research Committee of Faculty of Veterinary Medicine, South Valley University, Egypt, with approval number (No.77/04.10.2022).

Availability of data and material: The datasets collected during and/or analyzed for the current study are available from the corresponding author on reasonable request.

Conflicts of Interest: The authors declare no conflict of interest.

Funding: "This research received no external funding"

Author Contributions: Conceptualization, WFAE and MMF; Methodology, WFAE, MMF, NMH, ZA, and KAB; Software, WFAE, and MMF; Validation, WFAE; Formal analysis, WFAE, NMH, and KAB; Investigation, WFAE, MMF, ZA, and KAB; Resources, WFAE; Data curation, WFAE and MMF; Writing, original draft, WFAE; Writing review and editing and intellectual input, WFAE, MMF, NMH, ZA, HHA, CSR and KAB; Visualization, WFAE; Supervision, WFAE; Project administration, WFAE; Funding acquisition, WFAE, MMF, NMH, ZA, HHA and KAB.

Acknowledgments: The authors thank the Aquatic Animal Medicine Unit, Faculty of Veterinary Medicine, Assiut University, for technical assistance. Also, we would like to express our deepest appreciation to Prof. Ahmad Abd Elhady Elkamel, Professor and Department Head of Aquatic Animal Medicine and Management, Faculty of Veterinary Medicine, Assiut University, for his stimulating supervision and sincere efforts. We also thank The Electron Microscopy Unit at South Valley University for their technical assistance with scanning electron microscopic investigations**.**

Abbreviations

	Abbreviation	Extension
1	sp.	Species
2	18S rDNA	18S ribosomal DNA
3	*C. gariepinus*	*Clarias gariepinus*
4	18S SSU rDNA	18S small subunit ribosomal DNA
5	PCR	Polymerase chain reaction
6	G	Gram
7	mg/l	Milligram/liter
8	SEM	Scanning electron microscope
9	N	Number
10	Mm	Micrometer
11	kV	Kilovolt
12	H&E	Hematoxylin and eosin
13	nPCR	Nested PCR
14	(ERIB1 and ERIB10)	Universal eukaryotic primer pairs
15	(Myxospec-F and Myxospec-R)	Myxosporean specific 18S rDNA
16	µl	Microliter
17	mm	Millimeter
18	mM	Millimolar
19	Tris-HCl	Tris-hydrochloride
20	$(NH4)_2$ SO4	Ammonium sulfate
21	$MgCl_2$	Magnesium chloride
22	pmol	Picomole
23	BLASTn	Nucleotide Basic Local Alignment Search Tool
24	MEGA X software	Molecular evolutionary genetics analysis
25	min	Minute
26	N	North
27	E	East
28	RBCs	Red blood cells
29	NCBI	National Center for Biotechnology Information

30	bp	Base pair

References

Abdel-Baki A, Sakran T & Zayed E, (2011). Validity, impacts and seasonal prevalence of Henneguya species infecting catfish Clarias gariepinus from River Nile, Egypt. *Parasitology research*. **109**, 119-123.

Abdel-Ghaffar F, Abdel-Aziz A, Ezz El-Din N & Naas S, (1995). Light and electron microscopic studies on *Henneguya branchialis* Ashmawy et al., 1989 (Myxozoa: Myxosporea) infecting the catfish Clarias lazera in the River Nile, Egypt. *J Union Arab Biol*. **3**, 113-133.

Abdel-Ghaffar F, Abdel-Baki A-AS, Bayoumy EM, Bashtar A-R, Al Qurieshy S, Morsey KS, Alghamdy A & Mehlhorn H, (2008). Light and electron microscopic study on *Henneguya suprabranchiae* Landsberg, 1987 (Myxozoa: Myxosporea) infecting *Oreochromis niloticus*, a new host record. *Parasitology research*. **103**, 609-617.

Abdel-Ghaffar F, Morsy K, El-Ganainy S, Ahmed M, Gamal S, Bashtar A-R, Al Quraishy S & Mehlhorn H, (2015). Twelve myxosporean species of the family Myxobolidae infecting freshwater fishes of the River Nile, Egypt, with the description of four novel species. *Parasitology research*. **114**, 2985-2998.

Adriano EA, Arana S, Alves AL, Silva MRMd, Ceccarelli PS, Henrique-Silva F & Maia AAM, (2009). Myxobolus cordeiroi n. sp., a parasite of *Zungaro jahu* (Siluriformes: Pimelodiade) from Brazilian Pantanal: morphology, phylogeny and histopathology. *Veterinary Parasitology*. **162**, 221-229.

Adriano EA, Carriero MM, Maia AAM, Silva MRMd, Naldoni J, Ceccarelli PS & Arana S, (2012). Phylogenetic and host–parasite relationship analysis of *Henneguya multiplasmodialis* n. sp. infecting *Pseudoplatystoma* spp. in Brazilian Pantanal wetland. *Veterinary Parasitology*. **185**, 110-120.

Altschul SF, Madden TL, Schäffer AA, Zhang J, Zhang Z, Miller W & Lipman DJ, (1997). Gapped BLAST and PSIBLAST: a new generation of protein database search programs. *Nucleic Acids Res*. **25**, 3389−3402.

Ashmawy K, Abu El-Wafa S, Imam E & EL-Otify Y, (1989). Description of newly recorded Myxosporidian protozoa of freshwater fishes in Behera province, Egypt. *J Egypt Vet Med Ass*. **49**, 43-53.

Bancroft JD & Gamble M, (2008). Theory and practice of histological techniques. Elsevier health sciences.

Barta JR, Martin DS, Liberator PA, Dashkevicz M, Anderson JW, Feighner SD, Elbrecht A, Perkins-Barrow A, Jenkins MC & Danforth HD, (1997). Phylogenetic relationships among eight Eimeria species infecting domestic fowl inferred using complete small subunit ribosomal DNA sequences. *The Journal of parasitology*. 262-271.

Borkhanuddin MH, Cech G, Molnár K, Shaharom-Harrison F, Khoa TND, Samshuri MA, Mazelan S, Atkinson SD & Székely C, (2020). Henneguya (Cnidaria: Myxosporea: Myxobolidae) infections of cultured barramundi, Lates calcarifer (Perciformes: Latidae) in an estuarine wetlands system of Malaysia: description of Henneguya setiuensis n. sp., Henneguya voronini n. sp. and Henneguya calcarifer n. sp. *Parasitology research*. **119**, 85-96.

Burger M, Cribb T & Adlard R, (2006). Patterns of relatedness in the Kudoidae with descriptions of Kudoa chaetodoni n. sp. and K. lethrini n. sp.(Myxosporea: Multivalvulida). *Parasitology*. **134**, 669-681.

Chen W, Yang C & Zhao Y, (2020). Characterization of Myxidium spinibarba sp. nov.(Cnidaria, Myxosporea, Myxidiidae) from Spinibarbus sinensis (Bleeker, 1871) in Chongqing China. *Parasitology research*. **119**, 1485-1491.

Diab A, El-Bouhy Z, Sakr S & Abdel-Hadi Y, (2006). Prevalence of some parasitic agents affecting the gills of some cultured fishes in Sharkia, Damietta and Fayium governorates. *ISTA7, Arrizona, Mexico. hydrophila in fresh water fishes. ISTA7, Arrizona, Mexico*.

Eissa A, Abu Mourad I & Borhan T, (2006). A contribution on Myxosoma infection in cultured *Oreochromis niloticus* in Lower Egypt. *Nature and science*. **4**, 40-46.

Eissa I, Badran A, Mahmoud N & Osman H, (2002). Studies on henneguyosis in catfish, *Clarias gariepinus*. *Suez Canal Vet. Medic. J*. **1**, 415-424.

El-Mansy A, (2002). Immature stages and re-description of *Henneguya suprabranchiae* (Myxosporea: Myxobolidae), an intestinal parasite of the catfish *Clarias gariepinus* in the River Nile, Egypt. *Diseases of Aquatic Organisms*. **51**, 179-186.

El-Mansy A & Bashtar A-R, (2002). Histopathological and ultrastructural studies of *Henneguya suprabranchiae* Landsberg, 1987 (Myxosporea: Myxobolidae parasitizing the suprabranchial organ of the freshwater catfish *Clarias gariepinus* Burchell, 1822 in Egypt. *Parasitology research*. **88**, 617-626.

El-Matbouli M, Fischer-Scherl T & Hoffmann RW, (1992). Present knowledge on the life cycle, taxonomy, pathology, and therapy of some Myxosporea spp. important for freshwater fish. *Annual Review of Fish Diseases*. **2**, 367-402.

Emeish W, (2006). Gill affections in catfish (*Clarias gariepinus*) in Qena-Egypt. *MVSc thesis, South Valley University,Qena*.

Emeish WF, Fawaz MM, Al-Amgad Z & Hussein NM, (2022). Henneguya species infecting the gastrointestinal tract of Clarias gariepinus from the Nile River. *Diseases of Aquatic Organisms*. **148**, 43-56.

Endrawes M, (2001). Observations on some external and internal parasitic diseases in Nile catfishes. *Faculty of Veterinary Medicine, Zagazig University*.

Eszterbauer E, Sipos D, Kaján GL, Szegő D, Fiala I, Holzer AS & Bartošová-Sojková P, (2020). Genetic diversity of serine protease inhibitors in myxozoan (Cnidaria, Myxozoa) fish parasites. *Microorganisms*. **8**, 1502.

Ferguson JA, Atkinson SD, Whipps CM & Kent ML, (2008). Molecular and morphological analysis of Myxobolus spp. of salmonid fishes with the description of a new Myxobolus species. *Journal of Parasitology*. **94**, 1322-1334.

Fiala I, (2006). The phylogeny of Myxosporea (Myxozoa) based on small subunit ribosomal RNA gene analysis. *International Journal for Parasitology*. **36**, 1521-1534.

Fiala I, Bartošová-Sojková P & Whipps CM, (2015). Classification and phylogenetics of Myxozoa, In: Myxozoan evolution, ecology and development. Springer, pp. 85-110.

Griffin MJ, Khoo LH, Torrans L, Bosworth BG, Quiniou SM, Gaunt PS & Pote LM, (2009). New data on *Henneguya pellis* (Myxozoa: Myxobolidae), a parasite of blue catfish *Ictalurus furcatus*. *Journal of Parasitology*. **95**, 1455-1467.

Griffiths S, (2000). The use of clove oil as an anaesthetic and method for sampling intertidal rockpool fishes. *Journal of Fish Biology*. **57**, 1453-1464.

Grizzle JM & Rogers WA, (1976). Anatomy and histology of channel catfish. 1st edn. (ed. By Grizle, J.M. and Rogers, W.A.), Auburn university, Auburn, A.L., USA.

Katharios P, Varvarigos P, Keklikoglou K, Ruetten M, Sojan J, Akter M, Cascarano MC, Tsertou MI & Kokkari C, (2020). Native parasite affecting an introduced host in aquaculture: cardiac henneguyosis in the red seabream Pagrus major Temminck & Schlegel (Perciformes: Sparidae) caused by Henneguya aegea n. sp.(Myxosporea: Myxobolidae). *Parasites & vectors*. **13**, 1-14.

Kumar S, Stecher G, Li M, Knyaz C & Tamura K, (2018). MEGA X: molecular evolutionary genetics analysis across computing platforms. *Mol Biol Evol*. **35**, 1547−1549.

Landsberg JH, (1987). Myxosporean parasites of the catfish, Clarias lazera (Valenciennes). *Systematic Parasitology*. **9**, 73-81.

Lebelo S, Saunders D & Crawford T, (2001). Observations on blood viscosity in striped bass, *Morone saxatilis* (Walbaum) associated with fish hatchery conditions. *Transactions of the Kansas Academy of Science*. **104**, 183-194.

Lom J & Arthur J, (1989). A guideline for the preparation of species descriptions in Myxosporea. *Journal of Fish Diseases*. **12**, 151-156.

Lom J & Dykova I, (1995). Myxosporea (Phylum Myxozoa). Cited by Woo, P.T.K. (1995): fish diseases disorders. Vol. 1, Protozoan, Metazoan infections CAP international.

Lom J & Dyková I, (1992). Protozoan parasites of fishes. Elsevier Science Publishers.

Marwan A, Mohamed A, Ramadan N & Afifi S, (1998). Systematic and histopathological studies on some protozoan endoparasites in Clarias lazera from freshwater bodies in Assiut City. PhD thesis, Assiut University, Assiut, AR Egypt,

Morsy K, Abdel-Ghaffar F, Bashtar A-R, Mehlhorn H, Al Quraishy S & Abdel-Gaber R, (2012). Morphology and small subunit ribosomal DNA sequence of *Henneguya suprabranchiae* (Myxozoa), a parasite of the catfish *Clarias gariepinus* (Clariidae) from the River Nile, Egypt. *Parasitology research*. **111**, 1423-1435.

Naldoni J, Arana S, Maia AAM, Silva MRMd, Carriero MM, Ceccarelli PS, Tavares LER & Adriano EA, (2011). Host–parasite–environment relationship, morphology and molecular analyses of Henneguya eirasi n. sp. parasite of two wild Pseudoplatystoma spp. in Pantanal wetland, Brazil. *Veterinary Parasitology*. **177**, 247-255.

Noga EJ, (2010). Fish disease: diagnosis and treatment, 2nd edn. Wiley-Blackwell, Ames, IA.

Okamura B, Gruhl A & Bartholomew JL, (2015). An introduction to myxozoan evolution, ecology and development, In: Myxozoan evolution, ecology and development. Springer, pp. 1-20.

Osman H, (2001). Studies on parasitic gill affections in some cultured freshwater fishes. *Vet Thesis, MV Sc. Suez Canal Univ*.

Reed CC, Basson L & Van As LL, (2003). Myxozoans infecting the sharptooth catfish, Clarias gariepinus in the Okavango River and Delta, Botswana, including descriptions of two new species, Henneguya samochimensis sp. n. and Myxobolus gariepinus sp. n. *Folia parasitologica*. **50**, 183-189.

Sabri DM, Eissa IA, Danasoury MA & Khouraiba HM, (2010). Prevalence of *Henneguya branchialis* in catfish (*Clarias gariepinus*) in Ismailia, Egypt. *Int J Agric Bio*. **12**, 897-900.

Saleh RA, (2015). Myxosporidian infections in *Oreochromis niloticus* and *Clarias gariepinus PH D Thesis, Fac. Vet. Med., Assiut University*.

Salim KY & Desser SS, (2000). Descriptions and phylogenetic systematics of Myxobolus spp. from cyprinids in Algonquin Park, Ontario. *Journal of Eukaryotic Microbiology*. **47**, 309-318.

Soliman SA, Emeish WF & Abdel‐Hafeez HH, (2022a). Lactoferrin improves the immune response and resistance of silver carp, a hematological, light (histochemical and immunohistochemical), fluorescent, and scanning electron microscopic study. *Microscopy Research and Technique*. **85**, 3565-3581.

Soliman SA, Sobh A, Ali LA & Abd‐Elhafeez HH, (2022b). Two distinctive types of telocytes in gills of fish: A light, immunohistochemical and ultra‐structure study. *Microscopy Research and Technique*. **85**, 3653-3663.

Stilwell JM, Camus AC, Leary JH, Mohammed HH & Griffin MJ, (2019). Molecular confirmation of *Henneguya adiposa* (Cnidaria: Myxozoa) and associated histologic changes in adipose fins of channel catfish, *Ictalurus punctatus* (Teleost). *Parasitology research*. **118**, 1639-1645.

Tamura K & Nei M, (1993). Estimation of the number of nucleotide substitutions in the control region of mitochondrial DNA in humans and chimpanzees. *Mol Biol Evol*. **10**, 512−526.

Woodyard ET, Rosser TG, Stilwell JM, Camus AC, Khoo LH, Waldbieser G, Lorenz WW & Griffin M, (2022). New data on Henneguya postexilis Minchew, 1977, a parasite of channel catfish Ictalurus punctatus, with notes on resolution of molecular markers for myxozoan phylogeny. *Systematic Parasitology*. **99**, 41-62.